

# Evidences of a consolute critical point in the Phase Separation regime of $\text{La}_{5/8-y}\text{Pr}_y\text{Ca}_{3/8}\text{MnO}_3$ ( $y \sim 0.4$ ) single crystals

G. Garbarino and C. Acha\*

*Laboratorio de Bajas Temperaturas, Departamento de Física, FCEyN,  
Universidad de Buenos Aires, Ciudad Universitaria, (C1428EHA) Buenos Aires, Argentina*

P. Levy†

*Departamento de Física, CAC, Comisión Nacional de Energía Atómica,  
Gral Paz 1499, 1650 San Martín, Buenos Aires, Argentina*

T. Y. Koo

*Pohang Accelerator Laboratory, Pohang University of Science and Technology, Pohang, 790-784, S. Korea.*

S-W.Cheong

*Rutgers Center for Emergent Materials and Department of Physics and Astronomy, Rutgers University, New Jersey, USA*

(Dated: March 23, 2022)

We report on DC and pulsed electric field sensitivity of the resistance of mixed valent Mn oxide based  $\text{La}_{5/8-y}\text{Pr}_y\text{Ca}_{0.375}\text{MnO}_3$  ( $y \sim 0.4$ ) single crystals as a function of temperature. The low temperature regime of the resistivity is highly current and voltage dependent. An irreversible transition from high (HR) to a low resistivity (LR) is obtained upon the increase of the electric field up to a temperature dependent critical value ( $V_c$ ). The current-voltage characteristics in the LR regime as well as the lack of a variation in the magnetization response when  $V_c$  is reached indicate the formation of a non-single connected filamentary conducting path. The temperature dependence of  $V_c$  indicates the existence of a consolute point where the conducting and insulating phases produce a critical behavior as a consequence of their separation.

PACS numbers: 72.15.-v, 72.20.Ht, 75.40.-s, 75.47.Lx

## I. INTRODUCTION

A controlled mixture of charge-delocalized ferromagnetic (CD-F) and charge-ordered, antiferromagnetic (CO-AF) phases can be easily achieved in manganites that are in the phase separation (PS) regime. This was indeed observed in previous experiments in hole-doped manganites where the proportion of the CD-F phase was varied by changing temperature, electric or magnetic field, grain size or solely by waiting the evolution of the system to a different phase distribution<sup>1,2,3,4,5</sup>. Changes of several orders of magnitude were observed, for example, in the resistivity of the  $(\text{La}, \text{Pr}, \text{Ca})\text{MnO}_3$  compound, that were associated with the variation of the CD-F to CO-AF phase proportion, which determines the percolation scenario that governs the physics of this system<sup>6</sup>. The study of the properties of the electric-field-dependent phase distribution may reveal the nature of some intrinsic attributes of these PS materials, like their topological phase distribution<sup>7</sup>, their electrical transport mechanism<sup>8</sup> or their dynamical magnetic properties<sup>9</sup>.

In this paper we present the electric field sensitivity of resistivity and magnetization as a function of temperature in  $\text{La}_{5/8-y}\text{Pr}_y\text{Ca}_{3/8}\text{MnO}_3$  ( $y \sim 0.4$ ) single crystals (LPCMO). We show that the two phase percolation model, where the CD-F to CO-AF phase proportion increases as the applied electric field is increased, can only partially explain our results. A filamentary dielectric breakdown scenario gives instead a better understanding

of the measured properties, where the observed critical behavior of the breakdown field points out to the existence of a consolute point related to the separation of the CD-F and the CO-AF phases.

## II. EXPERIMENTAL

We have performed resistivity measurements as a function of temperature and electric field,  $\rho(T, V)$ , for temperatures in the  $4 \text{ K} \leq T \leq 300 \text{ K}$  range, and electric fields up to  $200 \text{ V cm}^{-1}$ , in  $\text{La}_{5/8-y}\text{Pr}_y\text{Ca}_{3/8}\text{MnO}_3$  (LPCMO,  $y \sim 0.4$ ) single crystals. Details of their synthesis and characterization can be found elsewhere<sup>10</sup>. Different contact configurations were used: a four terminal (4W) standard configuration for constant current measurements and a two wire (2W) configuration for high resistances (up to  $100 \text{ G}\Omega$  - using a Keithley 2400 SourceMeter) or for a constant voltage measurement. We also performed pulsed current-voltage measurements (I-V characteristics), by generating a single square pulse of increasing voltage (up to  $10 \text{ V}$ ) for  $20 \text{ ms}$  to  $2 \text{ s}$  (using an Agilent 33250A 80MHz Function/Arbitrary Waveform Generator) and determining the current by measuring the voltage in a calibrated resistance using an oscilloscope or directly with the SourceMeter for longer pulses. Temperature was measured by a small diode thermometer well thermally anchored to the sample. Most of the electrical transport experiments were performed without ap-

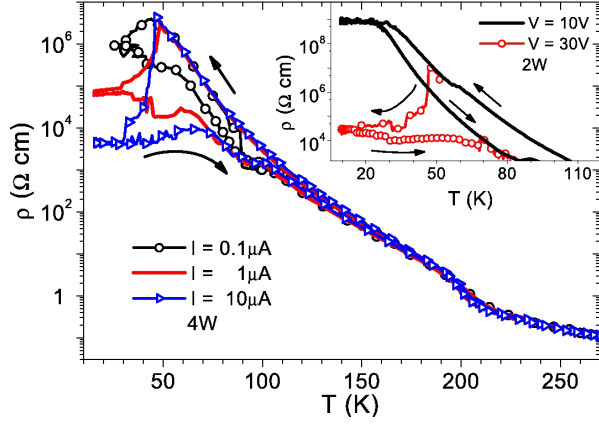


FIG. 1: Resistivity (4W, current controlled) of LPCMO as a function of temperature for various applied currents. The temperature evolution is indicated by arrows. The inset shows the 2W, voltage controlled resistivity.

plying an external magnetic field. When small magnetic fields were applied ( $H \sim 100$  Oe) in order to compare with magnetic measurements, we followed a zero field-cooled-warming procedure (ZFCW). Magnetization measurements, ZFCW and field-cooled-cooling (FCC) modes, were also performed as a function of temperature using a Lake-Shore 7400 VSM magnetometer to determine the magnetic response of these single crystals. Besides, in order to estimate the variation of the ferromagnetic volume fraction upon the application of an increasing electric field, magnetization measurements at a fixed temperature ( $T_0$ ) were also performed simultaneously with a 2W  $\rho(T_0, V)$  measurement.

### III. RESULTS AND DISCUSSION

Fig. 1 and its inset show the resistivity of a LPCMO ( $y \sim 0.4$ ) single crystal as a function of temperature for different constant currents and voltages (in the inset). For a low voltage range ( $V \leq 10$  V), the sample remains insulating down to low temperatures. A saturation is observed most probably due to the fact that the resistivity of the sample is beyond our measurement capability. When higher voltages are applied ( $10 \text{ V} \leq V \leq 100$  V), a metal-insulator like transition can be observed. A resistive drop of more than four orders of magnitude is obtained for the highest voltages as well as a characteristic temperature hysteresis for this system<sup>6</sup>. A similar behavior is observed for the current-controlled experiment.

Fig. 2 shows the voltage dependence of the resistivity ( $\rho(V)$ ) at a fixed temperature ( $\sim 20$  K), for a sample cooled in zero applied voltage (ZVC) and in zero magnetic field (ZFC). A very high and constant resistivity (HR) is measured as far as the voltage is increased up to a temperature dependent critical value ( $V_c(T)$ ), where a drop of more than four orders of magnitude is observed. This critical or breakdown voltage depends linearly with

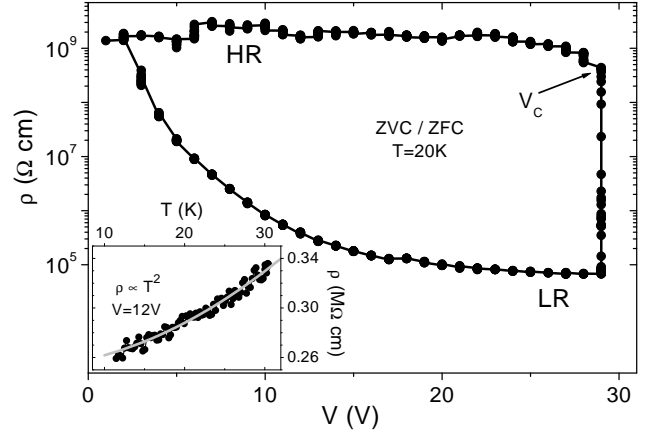


FIG. 2: 2W ZVC Resistivity of LPCMO as a function of the applied voltage at  $T=20$  K. The system evolves from a high resistance (HR) to a low resistance (LR) regime, after applying a voltage  $V \geq V_c$ . The inset shows a  $T^2$  dependence of the resistivity in the LR regime.

the increasing rate of the applied voltage. At this point, a time evolution of the resistivity is observed, which can be easily noticed by the reduction of the resistivity at a constant voltage  $V_c(T)$ . When the voltage is then decreased, the sample follows a different and more conducting path (LR), eventually reaching the same initial resistivity for low voltages. If the voltage is increased again, memory effects are observed as the sample remains in this LR path, showing a voltage reversible behavior and a  $T^2$  temperature dependence, as can be observed in the inset of Fig. 2. Similar results were obtained for temperatures  $T \leq 50$  K.

The temperature dependence of  $V_c(T)$  for a zero voltage cooled-zero voltage warming experiment (ZVC-ZVW) can be observed in the upper panel of Fig. 3, where the voltage was increased for each case at a 6V/min rate. In the lower panel, the temperature dependence of the ferromagnetic volume fraction ( $f$ ) is plotted for comparison. It should be noted that  $V_c \rightarrow 0$  for a temperature  $\sim 30$  K, which is lower than the one corresponding to the maximum of  $f$  ( $\sim 40$  K) and can be related to a change in the slope of the ZFC magnetization curve.

As when the sample reaches the LR regime the current considerably increases, flowing principally in a metallic percolation path, an additional Joule dissipation may occur. In this case, the shape of the highest voltage parts of these  $\rho(V)$  curves can be modified by overheating. To rule out this possibility, in particular for  $V \leq V_c$ , we performed pulsed  $\rho(V)$  measurements in the LR regime. As it is shown in Fig. 4, no time dependence can be observed for pulsed and DC voltages up to  $V < 10$  V, which can be interpreted as a lack of an overheating contribution to the shape of these  $\rho(V)$  characteristics.

In these conditions the obtained  $\rho$  shows a decrease with increasing  $V$ . This non-linear behavior in the LR regime also shows a particular power law dependence of

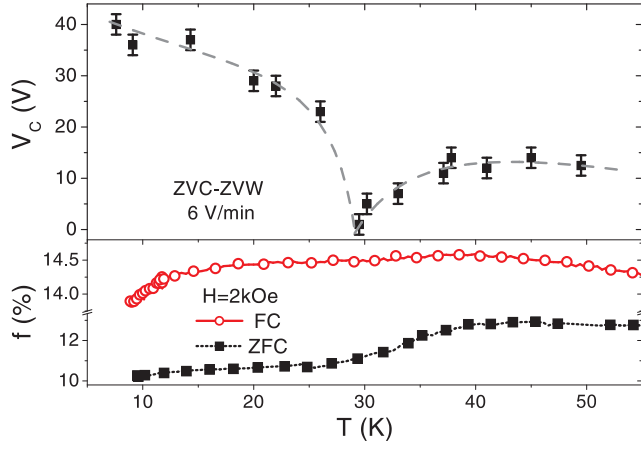


FIG. 3: Temperature dependence of the critical voltage ( $V_c$ ) for a zero-voltage-cooled experiment (upper panel). The lower panel shows the ferromagnetic volume fraction  $f$  as a function of temperature in the zero-field-cooled and the field-cooled-cooling modes.

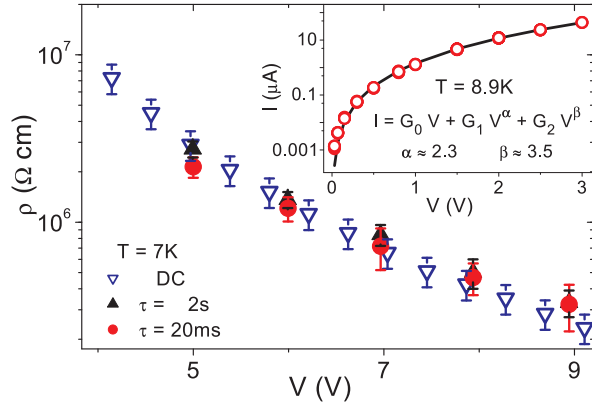


FIG. 4:  $\rho(V)$  curves measured in the LR regime applying single square pulses of different time width ( $\tau=20$  and  $2000$  ms) compared to DC measurements. The inset shows the particular  $I(V)$  characteristics of the LR regime.

the current ( $I$ ) with voltage ( $I \sim aV + bV^{7/3} + cV^{7/2}$ , as shown in the inset of Fig. 4). This particular behavior was previously observed analyzing the electrical transport properties of grain boundaries in manganites<sup>11,12,13,14</sup> and was interpreted within the framework described by the Glazman-Matveev (GM) theory<sup>15</sup>, which characterizes the case of multi-step tunneling of localized states within the grain boundary between two ferromagnetic conducting regions. The tunneling nature of the conducting process derived from our results indicates that the conducting percolation path established in the LR regime is not single connected.

In order to gain insight on the evolution of the CD-F volume fraction ( $f$ ) upon the application of a voltage  $V > V_c$ , we have measured simultaneously  $\rho(V)$  and  $M(V)$  at low magnetic fields ( $H=100$  Oe). Our results, obtained at  $T \sim 26$  K, are shown in Fig. 5. Surpris-

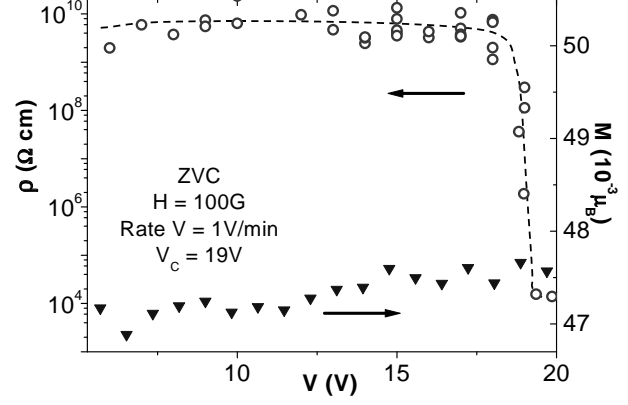


FIG. 5: Simultaneous measurements of the voltage dependence of the resistivity and the magnetization in a zero-voltage-cooled and zero-field-cooled experiment, performed at  $T \sim 26$  K. The dashed line is a guide to the eye.

ingly, although our magnetic measurement sensitivity let us to detect variations in  $f$  lower than 1%, no appreciable changes on the magnetization ( $M$ ) are detected when voltage produces the large resistivity drop at  $V_c$ . This lack of increase of the ferromagnetic volume fraction points toward the development of a filamentary percolation path, generated upon the increase of the applied voltage. This scenario is similar to the one usually observed during the dielectric breakdown of an insulator, where conducting defects increase with increasing voltage to finally produce a percolative path.

Another way to reach the same conclusion, namely that a 1D CD-F percolative path is established when the resistivity drop is observed (instead of a 2D or 3D network with an  $f$  higher than a critical percolation value  $f_c$ ), comes from the analysis of our resistivity measurements by using the general effective medium (GEM) equations (Eq. 1) developed by McLachlan<sup>16</sup> to describe the electric conductivity of a binary mixture of conducting and insulator materials:

$$f \frac{(\sigma_M^{1/t} - \sigma_E^{1/t})}{(\sigma_M^{1/t} + A\sigma_E^{1/t})} + (1-f) \frac{(\sigma_I^{1/t} - \sigma_E^{1/t})}{(\sigma_I^{1/t} + A\sigma_E^{1/t})} = 0, \quad (1)$$

where  $f$  is the volume fraction of the CD-F domains,  $\sigma_M$  and  $\sigma_I$  the conductivities of the metallic and insulating phases, respectively.  $\sigma_E$  is the effective conductivity that we measure,  $t$  and  $f_c$  are a critical exponent and the percolation threshold, respectively.  $A = \frac{1-f_c}{f_c}$ , and assuming that  $\sigma_M(T)=\sigma(T)$  of  $x=0$  and  $\sigma_I(T)=\sigma(T)$  of  $x=0.625$ , the values of  $f(V)$  can be calculated.

Within this GEM framework, both 2D or 3D percolation scenarios ( $t_{3D}=2$  or  $t_{2D}=1$  to  $1.4$ ,  $f_c=0.17$ ) yield to a variation of more than a 4% in  $f$  when the sample passes from the HR to the LR regime at  $V_c(T)$  ( $T < 33$  K).<sup>17</sup> This variation of the ferromagnetic fraction should be easily noticed in the  $M(V)$  measurements, which was

not the case, confirming the filamentary spatial distribution of the percolating path.

The PS scenario at low temperatures for this prototypical manganite, which can be depicted as small and isolated CD regions in a CO matrix, recalls, as we mentioned previously, the physics observed for dielectric breakdown in metal loaded dielectrics.<sup>18</sup> These materials were built as a mixture of a small fraction of a conducting component in an insulating matrix, which is an artificial representation of the intrinsic PS regime observed in manganites. Their dielectric breakdown field ( $V_{bd}$ ), related to a series of microscopic failures, depends on the conducting volume fraction, as described by an empirical relation of the form:

$$\frac{1}{V_{bd}(T)} = A(f) + (f_c - f)^{-\nu} \ln(L), \quad (2)$$

where  $A$  is a parameter,  $f$  the volume fraction of the CD-F domains,  $f_c$  the percolation threshold,  $\nu$  a critical exponent ( $\sim 0.85$  in 3D)<sup>19</sup> and  $L$  a linear dimension of the sample.

According to Eq. 2 and from the temperature dependence of the ferromagnetic volume fraction  $f$  obtained from the ZFC magnetization measurement, it is easy to notice that the expected  $V_{bd}$  should essentially follow the soft temperature variation of the ZFC magnetization and will not show, at any case, the quite unusual temperature dependence of  $V_c$  (showed in Fig. 3). This fact reveals the existence of another process, probably associated with a dielectric constant increase that may enhance considerably the local electric field ( $V_{bd} = \epsilon(T)V_c(T)$ ). Indeed,  $V_c(T)$  follows a critical behavior, described by a  $|T - T^*|^p$  dependence, as can be observed in Fig. 6. The best fitting parameters correspond to the temperature  $T^* \simeq 29.5$  K and to the critical exponent  $p \simeq 0.3$ .

Neglecting the small temperature dependence of  $V_{bd}$ , as  $\epsilon \sim V_c^{-1}$ , the obtained critical exponent may correspond to a divergence of the dielectric constant with a critical exponent  $p_\epsilon = -p \simeq -0.3$ . This particular divergence of the dielectric constant  $\epsilon$  was previously observed for binary liquid mixtures near the consolute critical point and can be associated with the Maxwell-Wagner effect<sup>20,21</sup>. This effect, related to the low frequency dielectric constant, results from the accumulation of conducting charges at the interface in the boundary between two phases of different conductivity. The effect is amplified near the consolute point, as the system, that behaves as homogenous far below this critical temperature, becomes heterogeneous (phase separated) for temperatures above  $T^*$ , with the occurrence of large-size phase fluctuations in a critical region. Remarkably, this framework seems to match very well with the PS scenario of manganites, where the CD-F and the CO-AF phases coexist in a determined temperature range. In our particular case, below  $T^*$  part of the CD-F and CO-AF phases become miscible, in accordance to the observed ferromagnetic volume fraction reduction, and show large fluctu-

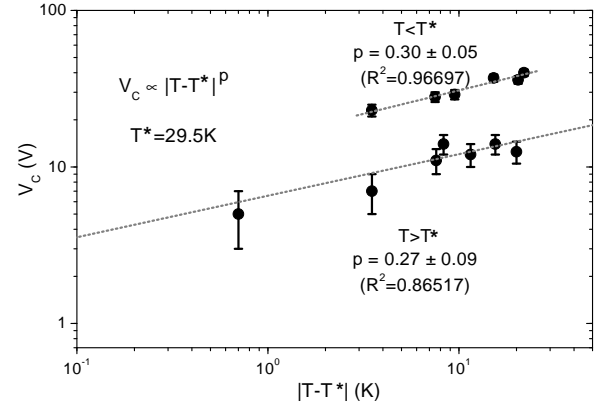


FIG. 6: Critical electric field as a function of the absolute relative temperature  $t = |T - T^*|$ . A critical exponent  $p \simeq 0.3$  and a  $T^* \simeq 29.5$  K are obtained from the best fits represented by the dotted lines.

ations between phase-separated and fully mixed (paramagnetic) volumes in a critical region near  $T^*$ . These CD-F volume fluctuations favor the formation of a percolation path when applying an external electric field, thus reducing the value needed to reach the critical field ( $V_c(T^*) \rightarrow 0$  V).

Recently, Ghivelder et al.<sup>9</sup>, showed for this particular manganite, the existence of a boundary between dynamic and frozen PS effects, with a peak in the magnetic viscosity at a temperature pretty much close to  $T^*$ . By similarity with the binary liquid mixtures, our results may indicate that the reported change in the PS dynamics can be explained by the appearance of this consolute-like point that should produce anomalies in many static and dynamic properties at  $T^*$ , as a consequence of the large fluctuations developed near that critical temperature<sup>22</sup>.

#### IV. CONCLUSIONS

We have shown that the low-temperature electrical resistivity of LPCMO single crystals is very sensitive to the magnitude of the applied electric field. The resistivity of a zero-electric-field-cooled sample can be varied more than four orders of magnitude by increasing the exciting voltage over a temperature dependent critical value ( $V_c(T)$ ). Our simultaneous electric and magnetic measurements indicate that a filamentary percolation path is established when the resistivity evolves irreversibly from a high to a low resistivity regime. The non-linear  $I - V$  characteristics obtained point out to the formation of a non-single connected path where multi-tunneling processes determine the electric transport properties of this regime. The presence of a consolute-like point at  $T^*$  was established by analyzing the critical behavior of  $V_c$ , that we associate with a Maxwell-Wagner effect. Thus, the presence of a consolute critical point sheds light on the

way that PS occurs, determining the particular behavior of the properties observed for this compound near the critical temperature.

## V. ACKNOWLEDGEMENTS

Partial financial support from a UBACyT (X198), AN-PCyT PICT 03-13517 and CONICET PIP 5609 grants

is acknowledged. Work at Rutgers was supported by the NSF-DMR-0520471 grant. GG acknowledges a scholarship from CONICET of Argentina. We are indebted to G. Pasquini for a critical reading of the manuscript and to D. Giménez, D. Melgarejo, C. Chilotte and E. Pérez-Wodtke for their technical assistance.

- 
- \* Also fellow of CONICET of Argentina. Fax: 0054-11-45763357; Electronic address: acha@df.uba.ar
- † Also fellow of CONICET of Argentina.
- <sup>1</sup> A. Asamitsu, Y. Tomioka, H. Kuwahara, and Y. Tokura, *Nature* (London) **388**, 50 (1997).
  - <sup>2</sup> P. Levy, F. Parisi, G. Polla, D. Vega, G. Leyva, H. Lanza, R. S. Freitas, and L. Ghivelder, *Phys. Rev. B* **62**, 6437 (2000).
  - <sup>3</sup> V. Hardy, A. Wahl, and C. Martin, *Phys. Rev. B* **64**, 064402 (2001).
  - <sup>4</sup> N. A. Babushkina, A. N. Taldenkov, L. M. Belova, E. A. Chistotina, O. Y. Gorbenko, A. R. Kaul, K. I. Kugel, and D. I. Khomskii, *Phys. Rev. B* **62**, R6081 (2000).
  - <sup>5</sup> N. K. Pandey, R. P. S. M. Lobo, and R. C. Budhani, *Phys. Rev. B* **67**, 054413 (2003).
  - <sup>6</sup> M. Uehara, S. Mori, C. H. Chen, and S.-W. Cheong, *Nature* (London) **399**, 560 (1999).
  - <sup>7</sup> J. Stankiewicz, J. Sesé, J. Garc'ia, J. Blasco, and C. Rillo, *Phys. Rev. B* **61**, 11236 (2000).
  - <sup>8</sup> V. Markovich, E. S. Vlahov, Y. Yuzhelevskii, B. Blagoev, K. A. Nenkov, and G. Gorodetsky, *Phys. Rev. B* **72**, 134414 (2005).
  - <sup>9</sup> L. Ghivelder and F. Parisi, *Phys. Rev. B* **71**, 184425 (2005).
  - <sup>10</sup> H. J. Lee, K. H. Kim, M. W. Kim, T. W. Noh, B. G. Kim, T. Y. Koo, S.-W. Cheong, Y. J. Wang, and X. Wei, *Phys. Rev. B* **65**, 115118 (2002).
  - <sup>11</sup> J. Klein, C. Höfener, S. Uhlenbruck, L. Alff, B. Büchner, and R. Gross, *Europhys. Lett.* **47**, 371 (1999).
  - <sup>12</sup> C. Höfener, J. B. Philipp, J. Klein, L. Alff, A. Marx, B. Büchner, and R. Gross, *Europhys. Lett.* **50**, 681 (2000).
  - <sup>13</sup> R. Gross, L. Alff, B. Büchner, B. H. Freitag, C. Höfener, J. Klein, Y. Lu, W. Mader, J. B. Philipp, M. S. R. Rao, et al., *J. Magn. Magn. Mater.* **211**, 150 (2000).
  - <sup>14</sup> K. B. Chashka, B. Fisher, J. Genossar, L. Patlagan, G. M. Reisner, and E. Shimshoni, *Phys. Rev. B* **63**, 064403 (2001).
  - <sup>15</sup> L. I. Glazman and K. A. Matveev, *Sov. Phys. JETP* **67**, 1276 (1988).
  - <sup>16</sup> D. S. McLachlan, *J. Phys. C: Solid State Phys.* **20**, 865 (1987).
  - <sup>17</sup> G. Garbarino, M. Monteverde, C. Acha, P. Levy, M. Quintero, T. Y. Koo, and S. W. Cheong, *Physica B* **354**, 16 (2004).
  - <sup>18</sup> P. D. Beale and P. M. Duxbury, *Phys. Rev. B* **37**, 2785 (1988).
  - <sup>19</sup> J. W. Essam, *Rep. Prog. Phys.* **43**, 53 (1980).
  - <sup>20</sup> J. Thoen, R. Kindt, W. V. Dael, M. Merabet, and T. K. Bose, *Physica A* **156**, 92 (1989).
  - <sup>21</sup> J. Hamelin, T. K. Bose, and J. Thoen, *Phys. Rev. A* **42**, 4735 (1990).
  - <sup>22</sup> P. C. Hohenberg and B. I. Halperin, *Rev. Mod. Phys.* **49**, 435 (1977).